Interaction with plasmid DNA of Hoechst-TACN conjugates

Massimo Tosolini,[a] Teresa Gianferrara,[a] Giuliana Mion,[a] Luca Dovigo,[b] Fabrizio Mancin,[c] Claudia Sissi,[b,*] and Paolo Tecilla.[d,*]

[a]*Department of Chemical and Pharmaceutical Sciences, University of Trieste, via Giorgieri 1, I-34127, Trieste, Italy*

[b]*Department of Pharmaceutical and Pharmacological Sciences, University of Padova, via Marzolo 5, Padova, Italy. E-mail: claudia.sissi@unipd.it*

[c]*Department of Chemical Sciences, University of Padova, via Marzolo 1, Padova, Italy.*

[d]*Department of Mathematic and Geosciences, University of Trieste, via Weiss 2, I-34127, Trieste, Italy. E-mail: ptecilla@units.it*

Interaction with plasmid DNA of Hoechst-TACN conjugates

A new family of conjugates between the Hoechst minor groove binder and the TACN metal ion ligand connected through hydrophobic alkyl or more hydrophilic oxyethyl linkers of different length has been prepared. The linkers are connected to the convex side of the curvature of the Hoechst skeletons thus forcing the TACN ligand to exit the minor groove and interact with the phosphate backbone of DNA. The conjugates and their Cu(II) and Zn(II) complexes interact strongly with DNA preserving the typical mode of binding of the Hoechst ligand. The strength of the interaction is strongly influenced by the nature of the linker, with the more hydrophobic being more efficient, and less by the presence and nature of the coordinated metal ion. In the case of the Zn(II) complex bearing a C6 linear alkyl linker a modest but reproducible acceleration of the hydrolytic cleavage of DNA has been observed which can be ascribed to the ability of the conjugate to deliver the hydrolytic subunit close to the DNA phosphate backbone.

Keywords: synthetic nucleases; Hoechst; TACN, Zn(II) and Cu(II) complexes, DNA cleavage

Introduction

In Nature the hydrolytic cleavage of P-O bonds in nucleic acids, DNA and RNA, is catalysed by a class of enzymes, named nucleases, which are ubiquitous and involved in many different regulation processes.[1] Nucleases are probably the more proficient enzymes Nature has evolved and catalyse the cleavage of DNA with impressive rate acceleration and sequence selectivity.[2] Natural restriction nucleases and engineered nucleases find also broad applications in the field of genomic and biotechnologies as tools for manipulating DNA.[3] Parallel to this, a long standing and growing effort has been made by chemists and supramolecular chemists toward the development of "artificial nucleases"[4] with the final aim to develop synthetic catalysts as new and

complementary tools for DNA editing and new antibiotic and chemotherapeutic drugs.[5]

The general design of artificial nucleases is based on the exploitation of the Lewis acidity of transition and lanthanide metal ions and theirs complexes which are the active catalysts of the phosphodiester bond cleavage.[6,7] However, reactivity and selectivity of simple complexes are usually modest also because of their low affinity for nucleic acids. During the years, several approaches have been exploited in order to improve reactivity and selectivity of these systems. They were based on the formation of more active multi-metallic catalysts[8] or on the conjugation of the metallic centre to DNA ligands such as, for example; major groove binders,[9] base pairs intercalators[10] or DNA and PNA fragments.[11,12] Somehow surprisingly, however, minor groove binders, which are an important class of DNA ligands,[13] have been very little exploited in conjugation with hydrolytic metal ions.[14] Some years ago the group of Qiao and Zhao reported conjugates between mono[15] or bimetallic[16] Zn(II) complexes with N-methylpyrrole-based oligopolyamides minor groove binders which cleaved DNA with moderate activity and selectivity toward A-T rich sequences and showed, in the case of the bimetallic complex, some preference for double strand cleavage. More recently, we described a family of conjugates between $(indole)_2$ or benzofurane-indole amides and the Zn(II)-triaminocyclohexane complex connected through flexible linkers of different length and nature.[17] The conjugates show high affinity for the DNA minor groove but were practically inactive in the hydrolytic cleavage of the macromolecule.

The above cited minor groove binder conjugates share a common structural topology in which the metal complex is attached trough a linear spacer to one extremity of the minor groove binder in a linear fashion. Molecular modelling of the interaction of these conjugates with DNA[17] shows the DNA binder tightly inserted in the DNA minor groove with the linker that follows the minor groove curvature establishing hydrophobic

interactions with the DNA. As a consequence, the metal complex is buried in the DNA minor groove away from the phosphate moieties (Figure 1A) and this conformation is unproductive or little productive from a hydrolytic point of view. A strategy to overcome this problem is to move the attachment point of the linker from the extremity to one side of the minor groove binder. In this way the linker should be forced to exit the minor groove allowing the interaction of the metal complex with the phosphate groups (Figure 1B). To text this hypothesis, we designed a new family of conjugates using as minor groove binder a derivative of Hoechst 33258,[18] which allows the attachment of the linker bearing the metal complex at the convex side of its curved skeleton thus forcing the linker to exit from the minor groove[19] (Figure 2). Here we report the synthesis, characterization and DNA interaction studies of this new class of compounds.

Figure 1

Results and Discussion

Design and synthesis of the Hoechst-TACN conjugates.

The structures of the Hoechst-TACN conjugates investigated in this work are reported in Figure 2. The Hoechst ligand was chosen because it is a representative minor groove binder with specificity to the $(A_3T_3)_2$ sequence[18] and because it was described the synthesis of a derivative bearing a carboxylic function on the first benzimidazole ring which is a convenient handle for connecting the linker bearing the hydrolytic unit.[19] Indeed, the carboxylic function is inserted on the convex side of the "banana shaped" Hoechst skeleton thus ensuring that the linker attached is forced toward the external side of the groove over the phosphate backbone (Figure 1B). As metal ion ligand the triazacyclononane (TACN) macrocycle was selected because it forms strong complexes

with Zn(II) which are efficient catalysts for the hydrolytic cleavage of model phosphate esters and plasmid DNA.[20] The TACN subunit was connected to the Hoechst skeleton *via* an amide bond using terminally amino functionalized flexible linkers of different length (from 4 to 8 atoms) and polarity (fully carbon or with some oxygen atoms) to vary the distance of the hydrolytic unit from the minor groove binder and, for the more polar linkers, to decrease the hydrophobic interactions with the DNA base pairs. Compound **5** differs from the others because the TACN is connected to the linker via a second amide bond which confers more rigidity to the system and may also, upon deprotonation of the amide nitrogen, be involved in the complexation of the metal ion. This type of linkage has been described in the preparation of self-assembled hydrolytic catalysts and the results indicate that the Zn(II) complex maintains its hydrolytic potency.[21]

Figure 2

The general synthetic pathway for the preparation of compounds **1**-**5** is reported in Scheme 1. The key intermediate is the Hoechst-COOH derivative which was prepared in a multistep synthesis starting from 3,4-dinitrobenzoic acid and 3-amino-5-chloro-2-nitrobenzoic acid, as reported.[19] In parallel the commercially available TACN was protected on two amines by statistical reaction with $(Boc)_2O$ giving the bis-protected macrocycle (**6**) in 50% yield. The non-protected amine of **6** was alkylated with the bromoalkyl(oxy)amines **7-10,** protected at the amino functions as benzyloxycabonyl derivatives, to give compounds **11**-**14**, or with benzylbromoacetate followed by removal of the benzyl group by catalytic hydrogenation to give **15**, respectively.[17] The carboxylic acid of **15** was then conjugated with the Cbz-monoprotected cadaverine using EDC and HOBT as condensing agent giving

compounds **16**. Removal of the Cbz protecting group by catalytic hydrogenation from all the linkers gives the free amine **17**-**21** which were coupled with Hoechst-COOH using BOP and HOBT as condensing agents and DIPEA as base. The final deprotection of the TACN amines with TFA at room temperature afforded the target compounds **1-5** as TFA salts.

Scheme 1

The Zn(II) and Cu(II) complexes of the conjugates **1-5** were prepared using a procedure optimized by us[10] in which the proper amount of the TFA salt of the conjugates is dissolved in a mixture of MeOH/water to obtain a millimolar solution. One equivalent of $Zn(NO_3)_2$ or $Cu(NO_3)_2$ was then added and the pH adjusted to about 7 by addition of a water solution of NaOH (Figure 3). The resulting solutions were directly used as stock solution for experiments with DNA. The formation of the complexes was confirmed by ESI-MS as illustrated in the case of the Zn(II) complex of compound **4** in Figure 3. The mass spectra show the absence of the free ligand at m/z = 663.3 and the formation of the (**4**-H^+)·Zn(II) complex at m/z = 729.3. The insets of Figure 3 show the good matching between the experimental (A) and calculated (B) isotopic cluster distribution of the metal complex. Similar results were obtained with all the other complexes.

Figure 3

Cleavage of plasmid DNA promoted by the Hoechst-TACN conjugates.

Starting from our previous experience with related conjugates, the interaction of the TACN conjugates and of their Zn(II) and Cu(II) complexes with plasmid DNA was preliminary investigated by agarose gel electrophoretic experiments. Increasing

amounts of the compounds were added to pBR 322 DNA (24 μM) in 20 mM HEPES, pH 7.1 and after 30 min incubation at 37°C the mixtures were loaded on an agarose gel. Figure 4 shows the results obtained with ligands **1**-**5** and with their Zn(II) and Cu(II) complexes.

Figure 4

By increasing the concentration of the conjugates the bands of the plasmid DNA progressively disappear from the gel while the nucleic acid appears to be trapped in the loading wells. This behaviour was already observed with the $(indole)_2$/TACH conjugates[17] and was correlated to an aggregation/precipitation of DNA induced by the binding of the conjugates to the macromolecule. The efficiency of this DNA fading effect was different among the five tested Hoechst conjugates and follows the ranking order: **1** > **5** >**2** >> **3** ≈ **4**. Significantly, it seems to correlate with the lipophilicity of the linker, with the compounds bearing only carbon linkers being by far more efficient in inducing the aggregation of the DNA respect to the compounds bearing oxyethyl linkers. The formation of the corresponding Cu(II) or Zn(II) metal complexes did not alter this trend to a significant extent. By comparing the DNA aggregation efficiency of the Hoechst/TACN conjugates with that of the $(indole)_2$/TACH conjugates bearing equivalent linkers these latter are almost twice as efficient.[17] Therefore, the phenomenon is further influenced, as expected, by the nature of the minor groove binder and by the topology of the conjugate.

The observed aggregation effect was reversible. Indeed, if after the 30 min incubation time at 37°C, the ligands or their metal complexes are forced to dissociate from the plasmid by addition of 1% SDS no significant impairment of the DNA electrophoretic mobility was observed. This is shown in Figure 4 in the case of ligand **5**

and its Zn(II) and Cu(II) complexes and similar results were obtained with all the other ligands and metal complexes.

After having demonstrated that the conjugates bind to DNA we investigated the ability of their Cu(II) and Zn(II) complexes to cleave the macromolecule. To asses it, we increased the incubation up to 24 h at 37°C and, after addition of 1% SDS to the reaction mixture, the reaction products were resolved by agarose gel electrophoresis. In the presence of hydrolytic activity by the metal complexes, the band of the supercoiled plasmid DNA should decrease with the concomitant appearance of the bands of the nicked and, eventually, linear forms.

As shown in Figure 5 for compound **1**, the free ligands showed a modest cleaving ability at the highest tested concentrations. A concentration dependent formation of nicked plasmid was detected also upon plasmid incubation with all Cu(II) complexes of conjugates **1**-**5**. However, this turned out to be not a specific cleavage promoted by the delivery of the TACN complexes towards the macromolecule. Indeed, as exemplified in Figure 5 in the case of the **1,** it is evident that after incubation with 100 μM Cu(II) the plasmid was completely nicked whereas, at same concentration of complex **1**-Cu(II), the supercoiled DNA was the most abundant form. This was confirmed also by kinetic experiment in which the plasmid was incubated for variable time with a constant concentration of metal complexes (15 μM) at 37 °C (Figure 5, panel B). Thus, it appeared that the complex formation actually reduced the DNA damage. Comparable results were obtained with all the complexes.

A different picture emerged with the Zn(II) complexes. Indeed, while the Zn(II) complexes of ligands **2**-**5** did not induced any DNA cleavage, complex **1**-Zn(II) caused a modest but reproducible increment of nicked plasmid which extent was concentration and time dependent (Figure 5, panel A and C, respectively). As reported in Figure 5 in

this case the cleavage, although modest, was detectable even at stoichiometric DNA metal complex concentrations. A control experiment in presence of TACN alone (100 μM), TACN-Zn(II) (100 μM) and TACN-Zn(II) (100 μM) with increasing concentration of free Hoechst shows the absence of any DNA cleavage highlighting the importance of the covalent linkage between the metal complex and the DNA ligand (Figure 5, panel D).

Figure 5

The different DNA cleavage behaviour between the Cu(II) and the Zn(II) complexes can be the results of the different reactivity of the two metal ions. With Cu(II) the background reaction is rather fast probably as a combination of hydrolytic and oxidative processes. On the contrary, Zn(II) is unable to promote the oxidative cleavage of DNA and the hydrolytic reaction is rather slow, almost undetectable in presence of the metal ion alone. Therefore, with copper the cleavage is dominated by the background reaction and the partial saturation of the metal ion coordination sites by the coordination with the TACN ligand results in an inhibition of the process. On the other hand, the absence of the background reaction with Zn(II) allows to detect a small cleavage rate increment. This effect is strongly dependent on the nature and the length of the linker and indeed is detectable only with conjugate **1** which has a long and hydrophobic linker which ensures a tight binding to DNA and enough conformational freedom to deliver the chelating unit towards the phosphate backbone. Other possible interpretations of this increased reactivity such as, for example, a proximity effect within ligand/DNA aggregates in which the metal ion attacks “intermolecularly” a phosphate unit of a filament different from that the corresponding Hoechst unit is bound to, appear less likely because no cleavage activity is observed with the Zn(II) complexes

of **5** and **2**, which are also able to aggregate the DNA, and with the family of the (indole)$_2$/TACH conjugates previously investigated[17] which are more effective than **1**-Zn(II) in aggregating the DNA. If an "aggregation induced cleavage" would be present, being a non-specific mechanism, some activity should have been observed also with the other conjugates. Moreover, cleavage is observed even at 15 μM **1**-Zn(II) concentration at which the aggregation should be not relevant (compare Panel C of Figure 5 with Figure 4). In any case, this modest but detectable hydrolytic cleavage of DNA promoted by the complex **1**-Zn(II) is a particularly relevant result for us because it is the first evidence of an increased cleavage efficiency of a minor groove binder Zn(II) complex respect to metal ion alone observed in the families of conjugates investigated by us.

Binding of the TACN conjugate 1 to double stranded DNA.

In order to properly describe the cleavage results, the binding of the Hoechst-TACN conjugate **1** to DNA was further investigated. Up to ligand concentration of 20 μM, the correlation between UV-Vis absorbance and ligand concentration did not significantly deviated from linearity thus reasonably ruling out severe aggregation of our conjugate in solution. Therefore, in the following experiments we used concentrations of **1** below 20 μM at which also the aggregation of DNA should be negligible (see Figure 4). Nevertheless, UV titrations of **1** with ctDNA, indicated the occurrence of multiple equilibria involving species with different optical properties. This was highlighted by the lack of well-defined isosbestic points and by a multi-phasic variation of the absorbance vs concentration (Figure 6 panels A and B). Fluorimetric titrations well paralleled this result (Figure 6, panels C and D). Indeed, low ctDNA concentrations caused a decrement of the intrinsic fluorescence of **1** that at DNA/**1** molar ration larger than 0.1 it was followed by a biphasic increment of the emission intensity.

All the above results well relate with literature data on the related Hoechst 33258.[22] Accordingly, the formation of not site selective complexes which drive the aggregation of the DNA can be proposed in the presence of an excess of the ligand. This fits with the observed electrophoretic profiles. At higher DNA/ligand ratio, the dye redistributes along the macromolecule and properly fits within the DNA minor groove. This binding mode is associated to a remarkable increment of the ligand fluorescence. Along this step, the ligand recognizes different nucleic acid sequences with variable affinity (a relevant preference for AT vs GC sites is reported for the related Hoechst 33258) and this justify the multi-phasic behaviour of the binding isotherms.

This binding model was further supported by the denaturation profile of a short double helix with a random sequence acquired in the presence of increasing **1** concentration (Figure 6, panel E). The ligand was confirmed to strongly bind it and to increase its overall thermal stability but, consistently, the resulting melting profile showed multiple transitions corresponding to the different complexes formed in solutions.

We found that the ligand complexation of Zn(II) or Cu(II) did not affect the binding mode of our conjugate.

Figure 6

To get rid of these problems and to have a better insight into the DNA binding mode of our bioconjugate to DNA, we performed CD titrations where we kept constant the concentration of ctDNA while increasing the concentration of **1** (Figure 7). Under this conditions, the ligand is expected to bind first to the sites with higher affinity. A strong positive induced dichroic signal appeared in the ligand absorption range that was consistent with the insertion of the ligands into the minor groove of the double helix. The first signal transition apparently reached saturation at a DNA (base pairs) ratios ≈

0.05, indicating that the main ligand binding sites on the DNA span about 20 base pairs. Higher ligand concentrations produced a further increment of this signal that fit with the occupancy of the minor groove at lower affinity sites. Increments of the buffer ionic strength (up to 500 mM NaCl) did not change this profile, thus confirming that none of these two binding events are extensively related to electrostatic interactions. Again, this overall picture perfectly match the one currently available for the interaction of Hoechts 33258 with ctDNA.[22]

Figure 7

Noteworthy, the metal complexes **1**-Zn(II) and **1**-Cu(II) produced an almost superimposable fingerprint thus supporting that the coordination of the metal ion does not rearrange the DNA binding mode. Therefore, we can conclude that neither the addition of the functionalized side-chain to the binding moiety nor the formation of the metal complexes prevent the recognition of the double helix or change the binding mode to a significant extent.

Inhibition of Toposiomerases activity promoted by the Hoechst-TACN conjugates.

It has been reported that the binding of Hoechst to DNA can impair its enzymatic processing by enzymes.[23] Thus we tested if the activity of a class of important DNA processing enzymes like as Toposiomerases can be inhibited by our ligands. Figure 8 shows the results obtained by adding increasing amount of **1** and its metal complexes to pBR322 (0.125 μg) in the presence of 1 U of human topoisomerase I or IIα. As expected we recorded a substantial suppression of Topo I and Topo II activity by **1** in the low micromolar concentrations range. Formation of the Zn(II) or Cu(II) metal

complexes did not revert this behaviour although they are modestly less efficient. This inhibition activity suggests that conjugate **1** may be cytotoxic because the cytotoxicity of the Hoechst ligand has been suggested to origin from the inhibition of this class of enzymes.[24] Further studies will be required to investigate this aspect.

Figure 8

Conclusions

We have here presented the synthesis of a new family of conjugates between a minor groove binder and a metal ion ligand and the study of the interaction between the conjugates and their Zn(II) and Cu(II) complexes with DNA. The conjugates were designed on the basis of results obtained with a different family of compounds[17] suggesting that a linear arrangement between minor groove binder/linker/metal complexes lead to efficient DNA binding but unproductive from a hydrolytic point of view because all the structure remains buried in the groove and the metal ion complex is unable to reach the phosphodiester linkage. Therefore, the topology of the conjugate was changed using a derivative of Hoechst as minor groove binder and attaching the linker laterally so that the metal ion complex should be able to exit the DNA groove being free to interact with the hydrolysable site. This hypothesis was verified at least in part. The new derivatives bind strongly to DNA preserving the typical mode of binding of Hoechst and its ability to interfere with the DNA enzymatic processing of enzymes such as Toposiomerases. However, despite the lateral attachment of the linker, that should minimize the interaction of the linker itself with the minor groove, the efficiency of the conjugates to aggregate DNA is strongly influenced by the nature of the linker with the more hydrophobic ones being the most effective and this may suggest, as observed with the $(indole)_2$/TACH conjugates previously investigated,[17] a similar trend

in the DNA affinity of the conjugates. On the other hand, the free, partially protonated, ligand and the metal complexes contribute almost equally to the binding of DNA suggesting a week electrostatic interaction between the charged moiety and the phosphate backbone. From a hydrolytic point of view with the complex **1**-Zn(II) a modest but reproducible and real cleavage of the DNA has been observed. On the contrary, all the other metal complexes are inactive or in the case of the Cu(II) complexes less active respect to the free metal ion. This can be interpreted on the basis that the hydrolytic effect is small and in the case of copper(II) the reaction is dominated by a background redox reactivity of the free metal ion while in the case of the less active Zn(II) ion some reactivity influenced by the nature and length of the linker can be evidenced. Apparently to ensure cleavage the linker needs to be long and hydrophobic possibly to allow the metal ion to reach the phosphodiester bond and to increase the interaction with the DNA. In any case this result is particularly interesting because it demonstrates that the design is correct in order to properly deliver the chelating unit towards the macromolecule and that new development are possible to increase activity and to overcome the inhibition effect observed with Cu(II). We have, however, to underline that the activity observed is low in particular when compared with similar systems based on intercalating ligands instead of minor groove binders.[10] This may suggest an active role of the DNA ligand in influencing the cleavage activity of the conjugates. Studies in this direction are underway to better define the role of the nature of the DNA ligand and of the structure of the conjugate in determining its DNA hydrolytic ability.

Experimental

Materials and general methods

All commercially available reagents were purchased from *Aldrich* and *Alfa Aesar* and used without purification unless otherwise mentioned. Solvents were purchased from *Aldrich*, *VWR*, *Fluka* and *Riedel*, and deuterated solvents from *Cambridge Isotope Laboratories* and *Aldrich*. Reactions were routinely monitored by thin-layer chromatography (TLC) on silica gel (precoated F_{254} *Merck* plates). Chromatography was performed on *Merck* silica gel 60F-254 (230÷400 Mesh) and the solvents employed were of analytical grade. NMR spectra were recorded on a Jeol 400 spectrometer (operating at 400 MHz for proton and at 100 MHz for carbon) or on Jeol X-270 (operating at 270 MHz for proton and at 67.8 MHz for carbon). Chemical shifts (δ) are reported in ppm using the solvent residual signal as an internal reference. Coupling constants (*J*) are quoted in Hz. Electrospray mass spectra were recorded on a Bruker Esquire 4000 ESI-MS instrument, and compounds were dissolved in methanol. Infrared spectra (IR) were measured on a Jasco FT/IR-200 instrument. Hoechst-COOH,[19] di-*tert*-butyl-[1,4,7]-triazacyclononane-1,4-dicarboxylate (diBoc-TACN, **6**),[25] 1,4-bis(*tert*-butyloxycarbonyl)-1,4,7-triazacyclononane-7-acetic acid (**15**),[25] *N*-benzyloxycarbonyl-6-bromo-1-hexylamine (**7**),[10] *N*-benzyloxycarbonyl-4-bromo-1-butylamine (**8**),[10] 2-[2-(*N*-benzyloxycarbonyl-2-aminoethoxy)ethoxy]-1-bromo-ethane (**9**),[17] 2-(*N*-benzyloxycarbonyl-2-aminoethoxy)-1-bromo-ethane (**10**),[17] 4,7-*N*,*N*-di-tert-butyloxycarbonyl-1-*N*-[6-(*N*-benzyloxycarbonyl)-aminohexyl]-1,4,7-triazacyclononane[26] (**11**) and 4,7-*N*,*N*-di-tert-butyloxycarbonyl-1-*N*-(6-aminohexyl)-1,4,7-triazacyclononane[26] (**17**) were prepared as reported.

Synthesis

*General synthesis of 4,7-N,N-di-tert-Butyloxycarbonyl-1-N-[ω-(N-benzyloxycarbonyl)-aminoalkyl/alkyloxy]-1,4,7-triazacyclononane derivatives (**12-14**).*

To a solution of 172 mg of diBoc-TACN (**6**, 0.5 mmol) in dry CH_3CN (15 mL) were added under argon flux 1.6 eq. of the appropriate amino bromo derivative (**8-10**) and 140 μl of *N*-diisopropylethylamine (DIPEA, 0.8 mmol). The obtained mixture was refluxed in a closed vial for 5 days and the reaction monitored by TLC (CH_2Cl_2/MeOH/NH_3 99:1:1). Then the solvent was removed under reduced pressure, the residue dissolved in $CHCl_3$ (30 mL) and washed three times with a 5% solution of $NaHCO_3$ (10 mL). The organic phase was dried over Na_2SO_4, concentrated and the crude residue was purified by flash chromatography (SiO_2, CH_2Cl_2/MeOH/NH_3 99:1:1) to afford the final compounds.

4,7-N,N-di-tert-Butyloxycarbonyl-1-N-[4-(*N*-benzyloxycarbonyl)-aminobutyl]-1,4,7-triazacyclononane (12). Yield 70%; Rf=0.5 (CH_2Cl_2/MeOH 9.5:0.5); ^{1}H-NMR, ($CDCl_3$) δ: 1.40-1.50 (m, 22H), 2.44 (m, 2H), 2.58 (m, 4H), 3.19-3.24 (m, 6H), 3.38-3.46 (m, 4H), 5.07 (s, 2H), 7.33 (m, 5H); ^{13}C-NMR ($CDCl_3$), δ: 25, 28, 28.5, 40.6, 49.1-55.8 (Boc-N-$(CH_2)_2$-N-Boc, linker-N-$(CH_2)_2$-N-Boc, -CH_2-N-TACN), 66.4, 79.4, 127.8-128.5 (Ph), 136, 155.4. ESI-MS (m/z): 535.6 [M+H$^+$];

4,7-*N,N*-di-*tert*-Butyloxycarbonyl-1-*N*-[2-[2-(*N*-benzyloxycarbonyl-2-aminoethoxy)ethoxy]ethyl]-1,4,7-triazacyclononane (13). Yield 38%; Rf=0.6 ($CHCl_3$/MeOH 9:1); ^{1}H-NMR, ($CDCl_3$) δ: 1.45 (s, 18H), 2.67-2.74 (m, 6H), 3.18-3.24 (m, 4H), 3.40-3.56 (m, 14H), 5.10 (s, 2H), 7.34 (m, 5H); ^{13}C-NMR ($CDCl_3$), δ: 28.5, 41.4, 49.7-56.4 (Boc-N-($\underline{C}H_2)_2$-N-Boc, linker-N-($\underline{C}H_2)_2$-N-Boc, -$\underline{C}H_2$-N-TACN), 66.5, 69.8, 69.9, 79.7, 128.1-128.7 (Ph), 136.3, 156.2. ESI-MS (m/z): 595.4 [M+H$^+$];

4,7-*N*,*N*-di-*tert*-Butyloxycarbonyl-1-*N*-[2-(*N*-benzyloxycarbonyl-2-aminoethoxy)ethyl]-1,4,7-triazacyclononane (14). Yield 89%; Rf=0.4 (CH_2Cl_2/MeOH 9.5:0.5); ^{1}H-NMR, ($CDCl_3$) δ: 1.45 (s, 18H), 2.68-2.74 (m, 6H), 3.17-3.25 (m, 4H), 3.35-3.48 (m, 10 H), 5.10 (s, 2H), 7.35 (m, 5H); ^{13}C-NMR ($CDCl_3$), δ: 28.6, 41.0, 49.6-56.1 (Boc-N-($\underline{C}H_2)_2$-N-Boc, linker-N-($\underline{C}H_2)_2$-N-Boc, -$\underline{C}H_2$-N-TACN), 66.6, 69.7, 79.5, 128.0-128.5 (Ph), 136.6, 156.4. ESI-MS (m/z): 551.5 [$M+H^+$], 573.5 [$M+Na^+$].

*Di-tert-butyl-7-[2-oxo-2-[5-(N-benzyloxycarbonyl)-1,5-butyldiamine]ethyl]-[1,4,7]-triazacyclononane-1,4-dicarboxylate (**16**).*

To a 5 mL DMF solution of 1,4-bis(*tert*-butyloxycarbonyl)-1,4,7-triazacyclononane-7-acetic acid (**15**, 50 mg, 0.13 mmol) were added EDCI (27 mg, 0.14 mmol), HOBt (22 mg, 0.14 mmol) and DMAP (17 mg, 0.14 mmol). After stirring at room temperature for 10 minutes 37 mg of Cbz-Cadaverine (0.15 mmol) dissolved in 3 mL of DMF were added and the stirring was maintained at room temperature for 2 days monitoring the reaction by TLC (CH_2Cl_2/MeOH 95:5). Then the reaction mixture was diluted with 50 mL of EtOAc and the organic phase was washed with water (3 x 30 mL), dried and evaporated at reduced pressure. The crude residue was purified by flash chromatography (CH_2Cl_2/MeOH 95:5) to afford 56 mg of pure **16** (yield 72%). Rf=0.15 (CH_2Cl_2/MeOH 9.5:0.5); ^{1}H-NMR, ($CDCl_3$) δ: 1.47 (m, 24H), 2.63 (m, 4H), 3.15-3.48 (m, 14H), 5.06 (s, 2H), 7.33 (m, 5H); ^{13}C-NMR ($CDCl_3$), δ: 171.8, 156.8, 156.7, 156.0, 155.9, 136.9, 128.7, 128.3, 128.2, 80.4, 80.1, 80.0, 77.4, 66.5, 63.5, 63.1, 54.9, 54.0, 53.8, 51.5, 50.7, 50.1, 48.9, 48.2, 40.7, 38.8, 29.7, 29.2, 28.5, 23.7. ESI-MS (m/z): 606.5 [$M+H^+$].

*General synthesis of conjugates between Hoechst-COOH and diBoc-TACN derivatives (**22-26**)*

To a methanol (5 ml) solution containing 0.15 mmol of the appropriate Z-protected ligands (**11**-**14**, **16**) a catalytic amount (10 mg) of 10% C-Pd was added. The resulting mixture was poured under hydrogen atmosphere overnight. The reaction was monitored by TLC ($CHCl_3$/MeOH/NH_3 9:1:0.1). Then the catalyst was filtered over celite and the solvent removed under reduced pressure affording the Z-deprotected derivatives **17**-**21** in quantitative yield. The compounds were used in the following step without further purification and characterization.

To a 10 mL DMF solution of Hoechst-COOH x 3HCl (0.87 mg, 0.15 mmol) BOP (331 mg, 0.75 mmol) and HOBt (115 mg, 0.75 mmol) were added. After stirring at room temperature for 10 minutes under argon flux a 5 mL DMF solution of 0.15 mmol of the above amines **17**-**21** and DIPEA (0.200 mL) was added and the stirring was maintained at room temperature for 2 hours monitoring the reaction by TLC. Then the reaction mixture was diluted with 50 mL of CH_2Cl_2 and the organic phase was washed with 5% $NaHCO_3$ (3 x 30 mL) and Brine (3 x 30 mL), dried and evaporated at reduced pressure. The crude residue was purified by flash chromatography (CH_2Cl_2/MeOH/NH_3 90:10:1) to afford the final compounds **22**-**26** in moderate yield.

Hoechst-C6-diBoc-TACN, (22). Yield 38%; Rf=0.45 (CH_2Cl_2/MeOH 7:3); ^{1}H-NMR, (CD_3OD) δ:1.33-1.40 (m, 22H), 1.56 (m, 2H), 1.74 (m, 2H), 2.36 (s, 3H,), 2.38-2.45 (m, 6H), 2.64 (m, 4H), 3.03-3.09 (m, 4H), 3.22 (m, 4H), 3.56 (m, 2H), 6.94 (d, 2H), 7.13 (s, 1H), 7.62 (d, 1H), 7.65 (s, 1H), 7.96 (d, 2H), 7.98 (d, 1H), 8.27 (s, 1H); ^{13}C-NMR (CD_3OD), δ: 168.4, 161.6, 157.5, 157.3, 157.2, 155.9, 153.9, 149.2, 129.8, 125.5, 122.8, 122.6, 121.8, 117.1, 115.4, 81.1, 81.0, 57.8, 57.7, 57.6, 56.0, 55.1, 54.9,

54.8, 54.7, 54.5, 51.7, 51.4, 51.2, 50.8, 50.5, 50.3, 46.0, 40.5, 30.4, 29.4, 29.1, 28.7, 28.3, 28.2. ESI-MS (m/z): 879.7 [M+H^+], 901.6 [M+Na^+].

Hoechst-C4-diBoc-TACN, (23). Yield 29%; Rf=0.56 (CH_2Cl_2/MeOH 7:3); ^{1}H-NMR, (CD_3OD) δ:1.32 (s, 18H), 1.67-1.74 (m, 4H), 2.44 (s, 3H), 2.58 (m, 6H), 2.75 (m, 4H), 3.10-3.17 (m, 4H), 3.26 (m, 4H), 3.59 (m, 2H), 6.95 (d, 2H), 7.17 (s, 1H), 7.64 (d, 1H), 7.67 (s, 1H), 7.96 (d, 2H), 7.99 (d, 1H), 8.27 (s, 1H); ^{13}C-NMR (CD_3OD), δ: 168.4, 161.6, 157.5, 157.4, 157.2, 155.9, 154.1, 149.1, 129.9, 125.4, 122.8, 122.7, 121.8, 117.1, 115.5, 81.1, 81.0, 57.6, 55.9, 55.3, 55.1, 55.0, 54.8, 54.7, 52.1, 51.4, 51.2, 51.0, 50.3, 49.8, 45.7, 40.5, 28.7, 28.4, 26.8. ESI-MS (m/z): 851.6 [M+H^+], 873.7 [M+Na^+].

Hoechst-TEG-diBoc-TACN, (24). Yield 25%; Rf=0.22 (CH_2Cl_2/MeOH 7:3); ^{1}H-NMR, (CD_3OD) δ: 1.31-1.36 (m, 18H), 2.39 (s, 3H), 2.44 (m, 6H), 2.70 (m, 4H), 2.97-3.03 (m, 4H), 3.20 (m, 4H), 3.38 (m, 2H), 3.66 (m, 2H), 3.77 (m, 4H), 3.82 (m, 2H), 6.96 (d, 2H), 7.21 (s, 1H), 7.66 (d, 1H), 7.70 (s, 1H), 7.98 (d, 2H), 8.10 (d, 1H), 8.33 (s, 1H); ^{13}C-NMR (CD_3OD), δ: 168.5, 161.6, 157.5, 157.4, 157.3, 155.8, 153.9, 149.2, 138.0, 129.90 125.4, 122.9, 122.6, 121.8, 117.1, 115.4, 81.0, 80.9, 71.7, 71.5, 70.9, 56.6, 56.0, 55.8, 55.6, 55.2, 54.8, 52.1, 51.4, 51.2, 50.9, 46.0, 40.8, 28.7. ESI-MS (m/z): 911.6 [M+H^+], 933.6 [M+Na^+].

Hoechst-DEG-diBoc-TACN, (25). Yield 38%; Rf=0.33 (CH_2Cl_2/MeOH 7:3); ^{1}H-NMR, (CD_3OD) δ: 1.25-1.33 (m, 18H), 2.39 (s, 3H), 2.54 (m, 4H), 2.69-2.77 (m, 6H), 2.91-3.05 (m, 4H), 3.17-3.20 (m, 8H), 3.63 (m, 2H), 3.75 (m, 4H), 6.95 (d, 2H), 7.17 (s, 1H), 7.65 (d, 1H), 7.68 (s, 1H), 7.97 (d, 2H), 8.03 (d, 1H), 8.30 (s, 1H); ^{13}C-NMR (CD_3OD), δ: 168.5, 161.6, 157.4, 157.3, 155.9, 154.0, 149.2, 138.1 129.9, 125.5, 122.8, 121.9, 117.1, 115.5, 103.2, 81.0, 80.9, 72.1, 71.5, 70.8, 57.2, 57.0, 56.8, 56.1,

56.0, 55.7, 55.6, 55.5, 54.8, 52.5, 51.5, 51.2, 50.9, 45.9, 41.0, 28.7, 28.6. ESI-MS (m/z): 867.6 [M+H^+].

Hoechst-C5-NHCOCH$_2$-diBoc-TACN, (26). Yield 45%; Rf=0.30 (CH_2Cl_2/MeOH 7:3); ^{1}H-NMR, (CD_3OD) δ: 1.33-1.38 (M, 18H), 1.58 (m, 2H), 1.65 (m, 2H), 1.78 (m, 2H), 2.39 (s, 3H), 2.53 (m, 4H), 2.69 (m, 4H), 3.03 (m, 16H), 3.58 (t, 2H), 6.92 (d, 2H), 7.11 (s, 1H), 7.63 (m, 2H), 7.62-7.65 (m, 3H), 8.22 (s, 1H); ^{13}C-NMR (CD_3OD), δ: 172.6, 166.7, 159.9, 156.4, 155.9, 155.7, 154.2, 152.3, 147.5, 128.3, 123.8, 120.9, 120.2, 115.5, 113.8, 80.1, 79.9, 79.8, 54.5, 54.3, 54.1, 53.4, 53.4, 50.0, 49.6, 49.5, 48.4, 44.4, 42.3, 39.0, 38.7, 29.0, 28.9, 27.3, 24.4, 17.9, 16.5, 11.7. ESI-MS (m/z): 922.5 [M+H^+], 944.5 [M+Na^+].

*General procedure for N-Boc deprotection (**1-5**)*

0.03 mmol of *N*-Boc protected derivatives (**22-26**) were dissolved in CH_2Cl_2 (2mL) and trifluoroacetic acid (2mL) was added. The mixture was stirred at room temperature for 1 h and the reaction monitored by TLC (CH_2Cl_2/MeOH/NH_3 90:10:1). Then the solvent was removed under reduced pressure and the residue was co-evaporated with toluene and ethyl ether several times to fully remove the TFA residues. The obtained trifluoroacetic salts **1-5** were characterized and utilized without any further purification.

Hoechst-C6-TACN, (1). Yield 95%; Rf=0 (CH_2Cl_2/MeOH 7:3); ^{1}H-NMR, (CD_3OD) δ: 1.40 (m, 2H), 1.54-1.60 (m, 4H), 1.77 (m, 2H), 2.73 (m, 2H), 2.98 (m, 7H), 3.15 (m, 2H), 3.03-3.09 (m, 4H), 3.25 (m, 6H), 3.52-3.57 (m, 6H), 3.65 (m, 2H), 3.82 (m, 2H), 6.96 (d, 2H), 7.21 (s, 1H), 7.56 (s, 1H), 7.73 (d, 1H), 7.89 (d, 2H), 8.14 (d, 1H), 8.22 (s, 1H); ^{13}C-NMR (CD_3OD), δ: 165.8, 163.12 151.3, 150.1, 146.9, 135.9, 133.6, 133.2, 129.7, 125.2, 124.3, 121.7, 114.7, 113.8, 112.6, 111.5, 102.4, 55.2, 53.2, 43.0, 42.2, 41.6, 39.3, 29.2, 26.7, 26.6, 24.4. ESI-MS (m/z): 679.5 [M+H^+].

Hoechst-C4-TACN, (2). Yield 94%; Rf=0 (CH_2Cl_2/MeOH 7:3); ^{1}H-NMR, (CD_3OD) δ: 1.73 (m, 4H), 2.83 (m, 2H), 3.0 (m, 7H), 3.18 (m, 2H), 3.27 (m, 4H), 3.55-3.60 (m, 6H), 3.67 (m, 2H), 3.86 (m, 2H), 7.01 (d, 2H), 7.28 (s, 1H), 7.64 (s, 1H), 7.82 (d, 1H), 7.96 (d, 2H), 8.22 (d, 1H), 8.34 (s, 1H); ^{13}C-NMR (CD_3OD), δ: 165.9, 163.2, 151.6, 150.3, 147.1, 135.9, 133.4, 129.8, 125.0, 124.6, 121.7, 114.9, 113.9, 112.7, 111.8, 102.6, 65.4, 54.6, 53.3, 48.4, 43.1, 42.2, 41.7, 39.0, 27.1, 21.7, 14.0. ESI-MS (m/z): 651.5 [$M+H^+$].

Hoechst-TEG-TACN, (3). Yield 97%; Rf=0 (CH_2Cl_2/MeOH 7:3); ^{1}H-NMR, (CD_3OD) δ: 2.78 (m, 2H), 2.95 (m, 4H), 2.99 (s, 3H), 3.19-3.25 (m, 6H), 3.60-3.82 (m, 16H), 6.94 (d, 2H), 7.22 (s, 1H), 7.56 (s, 1H), 7.72 (d, 1H), 7.87 (d, 2H), 8.15 (d, 1H), 8.21 (s, 1H); ^{13}C-NMR (CD_3OD), δ: 166.1, 163.2, 151.2, 149.9, 147.1, 135.6, 133.2, 131.9, 129.8, 124.6, 121.4, 117.4, 114.9, 113.9, 112.3, 111.7, 102.5, 69.9, 69.8, 69.6, 67.7, 53.8, 53.2, 48.6, 44.2, 42.8, 42.2, 39.2. ESI-MS (m/z): 711.5 [$M+H^+$].

Hoechst-DEG-TACN, (4). Yield 95%; Rf=0 (CH_2Cl_2/MeOH 7:3); ^{1}H-NMR, (CD_3OD) δ: 2.91 (m, 2H), 3.0 (m, 7H), 3.18 (m, 6H), 3.57 (m, 4H), 3.67 (m, 2H), 3.75 (m, 2H), 3.79 (m, 4H), 3.87 (m, 2H), 7.00 (d, 2H), 7.30 (s, 1H), 7.64 (s, 1H), 7.83 (d, 1H), 7.96 (d, 2H), 8.23 (d, 1H), 8.34 (s, 1H); ^{13}C-NMR (CD_3OD), δ: 166.1, 163.3, 151.6, 150.1, 147.3, 135.7, 133.4, 132.1, 129.9, 124.7, 124.6, 121.6, 115.0, 114.0, 112.5, 112.0, 102.6, 69.6, 67.8, 53.9, 53.2, 48.2, 43.6, 42.2, 39.3, 29.4. ESI-MS (m/z): 667.5 [$M+H^+$].

Hoechst-C5-NHCOCH$_2$-TACN, (5). Yield 94%; Rf=0 (CH_2Cl_2/MeOH 7:3); ^{1}H-NMR, (CD_3OD) δ: 1.51 (m, 2H), 1.64 (m, 2H), 1.77 (m, 2H), 2.99 (s, 3H), 3.02 (m, 4H), 3.17-3.28 (m, 7H), 3.50 (s, 2H), 3.54 (t, 2H), 3.66 (m, 6H), 3.84 (m, 2H), 6.94 (d, 2H), 7.21 (s, 1H), 7.56 (s, 2H), 7.74 (d, 2H), 7.88 (d, 2H), 8.11 (d, 1H), 8.22 (s, 1H); ^{13}C-NMR (CD_3OD), δ: 172.9, 165.6, 163.2, 151.4, 149.7, 147.3, 135.4, 133.4, 131.9,

129.8, 124.6, 121.7, 117.2, 114.9, 113.9, 112.3, 111.9, 102.2, 63.5, 55.7, 54.4, 53.71, 53.3, 53.2, 49.6, 48.4, 44.7, 43.2, 42.2, 39.3, 39.2, 28.9, 28.5, 24.1, 17.8, 17.3, 11.7. ESI-MS (m/z): 722.5 [$M+H^+$].

Electrophoretic procedure for DNA interaction study

Stock solutions of the TACN minor groove binders conjugates **1**-**5** (0.5 – 1 mmol) were prepared in H_2O/CH_3OH 2:1. The ligand was diluted in the proper solvent mixture, one equivalent of $Zn(NO_3)_2$ or $Cu(NO_3)_2$ in water was added and the pH was corrected to 7 by addition of NaOH. The methanol content in the final reaction mixtures was always lower than 4%. DNA interaction was monitored using pBR 322 (Gibco BRL) in 20 mM HEPES, pH 7.1. Reactions were performed by incubating DNA (24 μM residues) at 37°C in the presence/absence of increasing amounts of ligand and corresponding metal complex for the indicated time. Reaction products were resolved on a 1% agarose gel in TAE buffer (40 mM TRIS base, 20 mM, acetic acid, 1 mM EDTA). To properly check for ligand-mediated DNA damages, samples were prepared as above reported but, before loading, the reaction mixture was added of 1% SDS to dissociate the ligands from DNA. The resolved bands were visualized by ethidium bromide staining and photographed on a Geliance apparatus.

UV-VIS and fluorometric titrations

UV-VIS and fluorometric titrations were performed with a Perkin-Elmer λ20 and Agilent Cary Eclipse, respectively. Binding was followed by addition of increasing amounts of ctDNA to a freshly prepared ligand solution in 20 mM HEPES, pH 7.1. Experimental data were analyzed in terms of relative variation of the absorbance/fluorescence at a constant wavelength as a function of DNA concentration.

Fluorescence melting studies

Melting experiments were performed in a Roche LightCycler, using an excitation source at 488 nm and recording the fluorescence emission at 520 nm using as target DNA a double stranded DNA (5'- GGATGTGAGTGTGAGTGTGAGG) with Dabcyl at the 5 ′and FAM at the 3' end of the complementary strand. Mixtures (20 µL) contained 0.25 µM of target DNA and increasing concentrations of tested derivatives (0-10 µM) in 50 mM potassium buffer (10 mM LiOH, pH 7.4 with H_3PO_4, 50 mM KCl). Readings were taken while applying a 0.2 °C/min heating rate. Each curve was repeated at least three times and errors were ± 0.4 °C.

CD measurements

Circular dichroism spectra were recorded at 25 °C using 1 cm path length quartz cells on a Jasco J 810 spectropolarimeter equipped with a peltier temperature controller. CD spectra were recorded on samples containing 80 µM ctDNA and increasing ligands concentrations in 20 mM HEPES, pH 7.1. The reported spectrum of each sample represents the average of 3 scans. Observed ellipticities were converted to mean residue ellipticity [θ] = deg x cm^2 x $dmol^{-1}$ (Mol. Ellip.).

Topoisomerase inhibition

0.125 µg of pBR322 (Inspiralis) were incubated with increasing concentrations (0.5-200 µM) of tested compounds for 1 hour at 37 °C in the presence/absence of 1 U of human topoisomerase I or IIα (Inspiralis) in the required buffer (1X). Reaction products were resolved on a 1% agarose gel prepared in 1X TAE (10mM Tris 1mM EDTA, 0.1% acetic acid, pH 8.0). After the electrophoretic run (5 V/cm for about 90 min) the DNA bands were visualized by ethidium bromide staining, photographed and quantified using

a Geliance 2000 apparatus.

Acknowledgements

The authors thank dr. Ilaria Furlan for her involvement in part of the synthetic work. This work was supported by the MSCA-ITN MMBIO (721613) project.

References

(1) Yang, W. *Q Rev. Biophys.* **2011**, *44*, 1-93.

(2) Wolfenden, R. *Chem. Rev.* **2006**, *106*, 3379-3396.

(3) Gaj, T.; Gersbach, C. A.; Barbas, C. F. *Trends Biotechnol.* **2013**, *31*, 397-405.

(4) Mancin, F.; Scrimin, P.; Tecilla, P. *Chem. Commun.* **2012**, *48*, 5545-5559.

(5) Yu, Z.; Cowan, J. A *Curr. Opin. Chem. Biol.* **2018**, *43*, 37-42.

(6) Mancin, F.; Scrimin, P.; Tecilla, P.; Tonellato, U. *Chem. Commun.* **2005**, 2540-2548.

(7) Mancin, F.; Tecilla, P. *New J. Chem.* **2007**, *31*, 800–817.

(8) Brown, R. S.; Lu, Z.-L.; Liu, C. T.; Tsang, W. Y.; Edwards, D. R.; Neverov, A. *J. Phys. Org. Chem.* **2010**, *23*, 1–15.

(9) Copeland, K. D.; Fitzsimons, M. P.; Houser, R. P.; Barton, J. K. *Biochemistry* **2002**, *41*, 343–356.

(10) Boseggia, E.; Gatos, M.; Lucatello, L.; Mancin, F.; Moro, S.; Palumbo, M.; Sissi, C.; Tecilla, P.; Tonellato, U.; Zagotto, G. *J. Am. Chem. Soc.* **2004**, *126*, 4543–4549.

(11) Lönnberg, T.; Aiba, Y.; Hamano, Y.; Miyajima, Y.; Sumaoka, J.; Komiyama, M. *Chem. Eur. J.* **2010**, *16*, 855–859.

(12) Zelder, F. H.; Mokhir, A. A.; Krämer, R. *Inorg. Chem.* **2003**, *42*, 8618–8620.

(13) Kawamoto, Y.; Bando, T.; Sugiyama, H. *Bioorg. Med. Chem.* **2018**, *26*, 1393–1411.

(14) Wang, J.-T.; Xia, Q.; Zheng, X.-H.; Chen, H.-Y.; Chao, H.; Mao, Z.-W.; Ji, L.-N. *Dalton Trans.* **2010**, *39*, 2128–2136.

(15) Li, C.; Qiao, R.-Z.; Wang, Y.-Q.; Zhao, Y.-F.; Zeng, R. *Bioorg. Med. Chem. Lett.* **2008**, *18*, 5766–5770.

(16) Li, C.; Du, C.; Tian, H.; Jiang, C.; Du, M.; Liu, Y.; Qiao, R.-Z.; Jia, Y.-X.; Zhao, Y.-F. *Chem. Eur. J.* **2010**, *16*, 12935–12940.

(17) Sissi, C.; Dovigo, L.; Greco, M. L.; Ciancetta, A.; Moro, S.; Trzciński, J. W.; Mancin, F.; Rossi, P.; Spalluto, G.; Tecilla, P. *Tetrahedron*, **2017**, *73*, 3014–3024.

(18) Spink, N.; Brown, D. G.; Skelly, J. V.; Neidle, S. *Nucleic Acids Res*. **1994**, *22*, 1607-1612.

(19) Tanada, M.; Tsujita, S.; Sasaki, S. *J. Org. Chem.* **2006**, *71*, 125-134.

(20) Bonfá, L.; Gatos, M.; Mancin, F.; Tecilla, P.; Tonellato, U. *Inorg. Chem.* **2003**, *42*, 3943-3947.

(21) Mancin, F.; Prins, L. J.; Pengo, P.; Pasquato, L.; Tecilla, P.; Scrimin, P. *Molecules* **2016**, *21*, 1014.

(22) a) Rahimian, M.; Miao, Y.; Wilson, W. D *J. Phys. Chem. B.* **2008**, *112*, 8770-8778; b) Stokke, T.; Steen, H. B. *J. Histochem. Cytochem.* **1985**, *33*, 333-338; c) Loontiens, F. G.; Regenfuss, P.; Zechel, A.; Dumortier, L.; Clegg, R. M. *Biochemistry* **1990**, *29*, 9029-9039.

(23) a) McHugh, M. M.; Woynarowski, J. M.; Sigmund, R. D.; Beerman, T. A. *Biochem. Pharmacol.* **1989**, *38*, 2323-2328; b) Woynarowski, J. M.; Sigmund, R. D.; Beerman, T. A. *Biochemistry* **1989**, *28*, 3850-3855.

(24) Baraldi, P. G.; Bovero, A.; Fruttarolo, F.; Preti, D.; Tabrizi, M. A.; Pavani, M. G.; Romagnoli, R. *Med. Res. Rev.* **2004**, *24*, 475-528.

(25) Mion, G.; Gianferrara, T.; Bergamo, A.; Gasser, G.; Pierroz, V.; Rubbiani, R.; Vilar, R.; Leczkowska, A.; Alessio, E. *ChemMedChem* **2015**, *10*, 1901-1914.

(26) Bonora, G. M.; Drioli, S.; Felluga, F.; Mancin, F.; Rossi, P.; Scrimin, P.; Tecilla, P. *Tetrahedron Lett.* **2003**, *44*, 535-538.

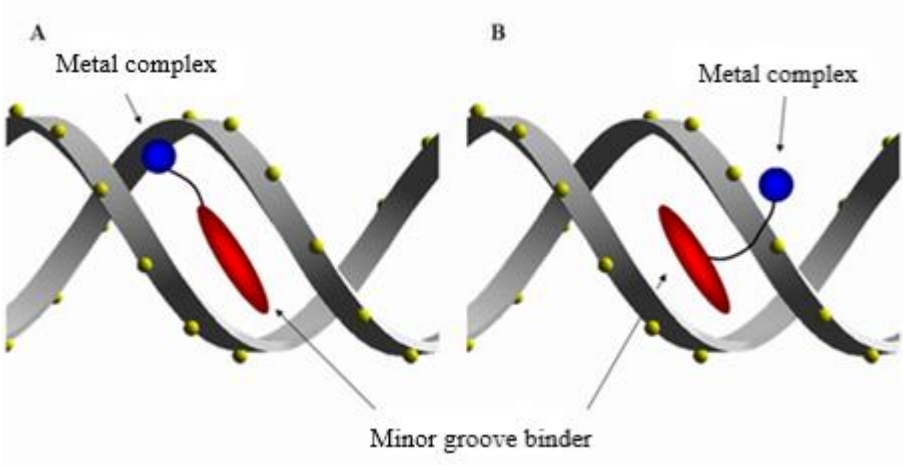

Figure 1. Cartoon of the interaction between metal complex/minor groove binder conjugates and DNA. The linear arrangement of the minor groove binder/linker/metal complex hampers the interaction of the hydrolytic unit with the phosphates (1A) while the lateral attachment of the linker to the minor groove forces the metal complex to exit from the groove and favours its interaction with the phosphates (1B).

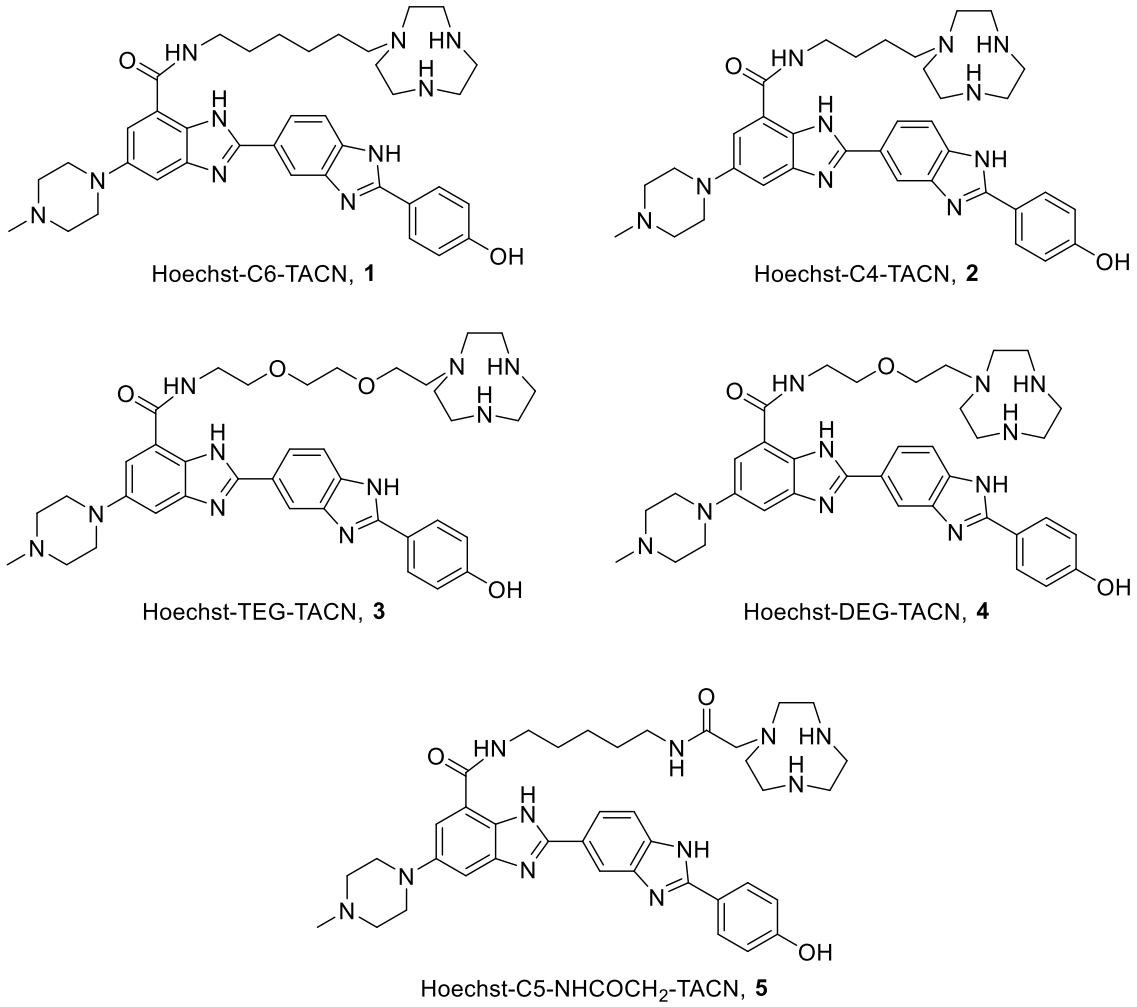

Figure 2. Structures of the Hoechst-TACN conjugates synthesized.

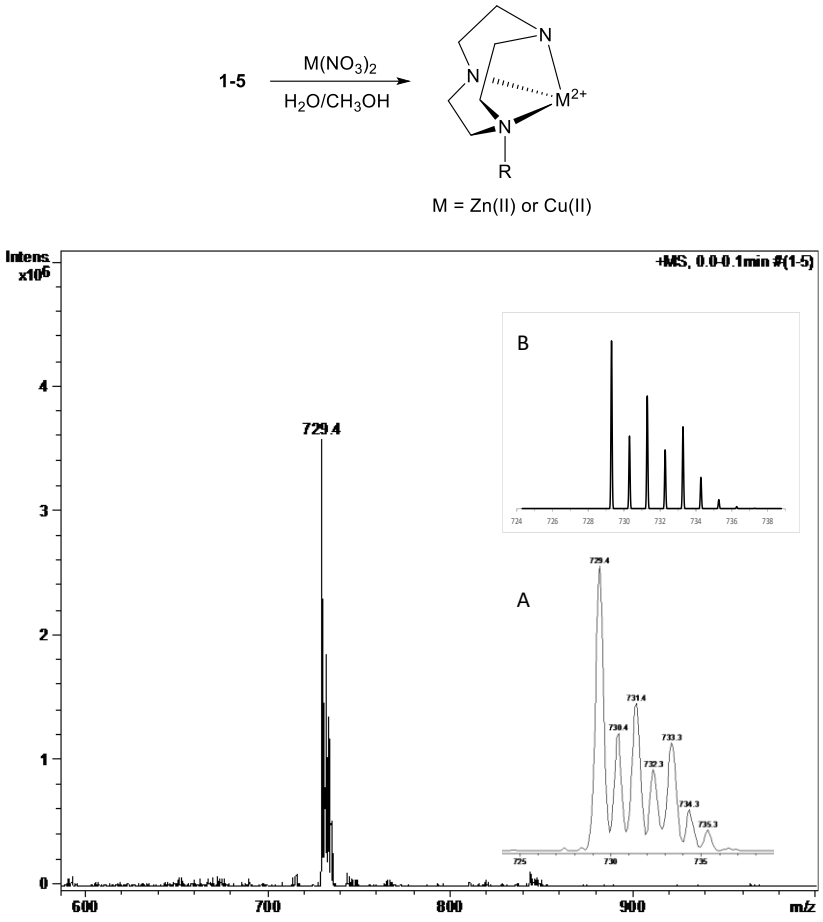

Figure 3. Formation of the metal complexes of compounds **1-5** (top) and ESI-MS spectra of the complex between compound **4** and $Zn(NO_3)_2$ (bottom). The insets show the experimental (A) and calculated (B) isotopic cluster distribution for the complex with formula $(4\text{-}H^+)\cdot Zn(II)$.

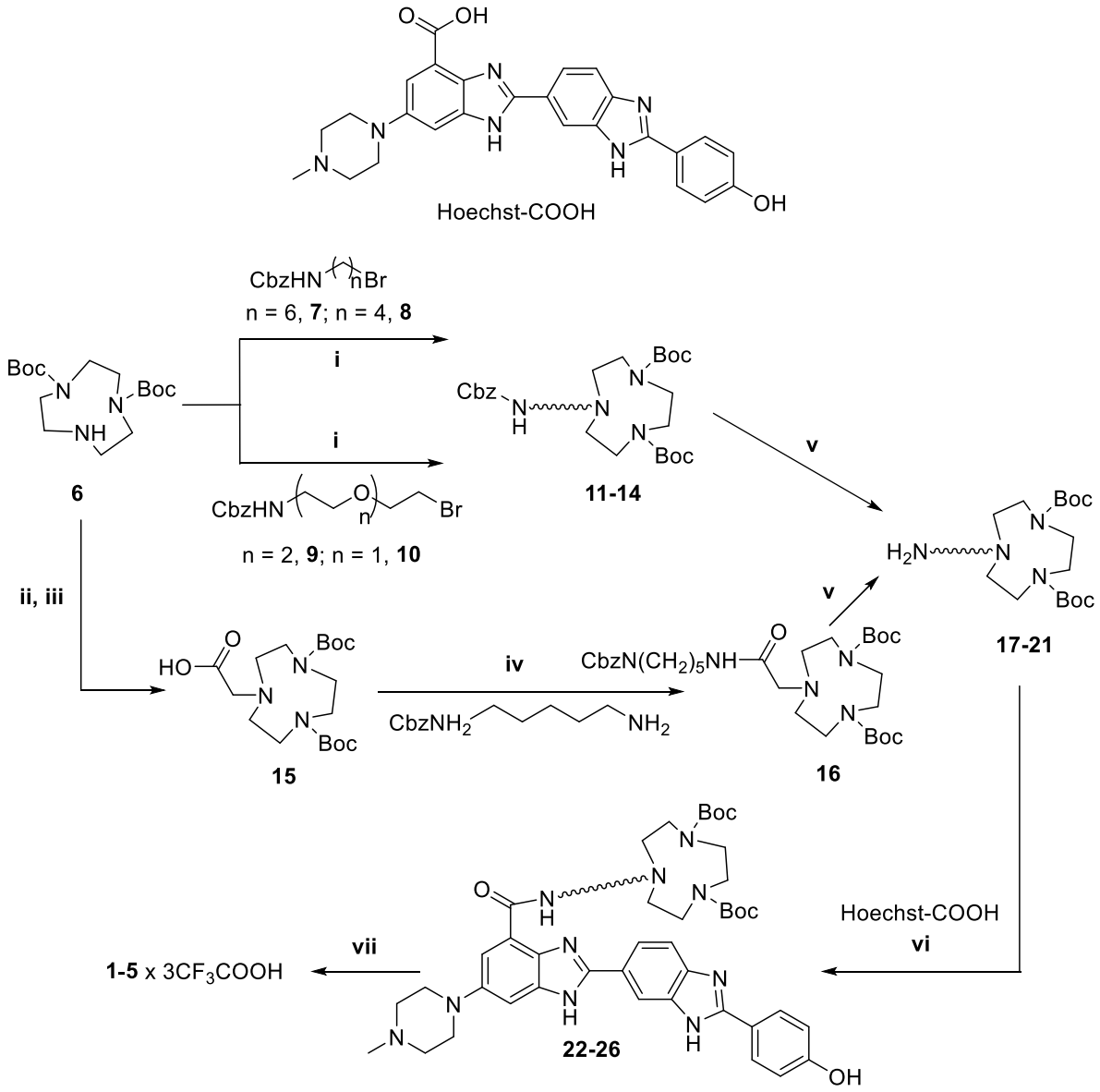

Scheme 1. Reagents: i: CH_3CN, DIPEA, reflux; ii: Benzylbromoacetate, CH_3Cl, TEA, rt; iii: H_2, C-Pd 10%, CH_3OH, rt; iv: EDC, HOBT, DMAP, DMF, rt; v: H_2, C-Pd 10%, CH_3OH, rt; vi: BOP, HOBT, DIPEA, DMF, rt; vii: CH_2Cl_2/TFA 1:1, rt.

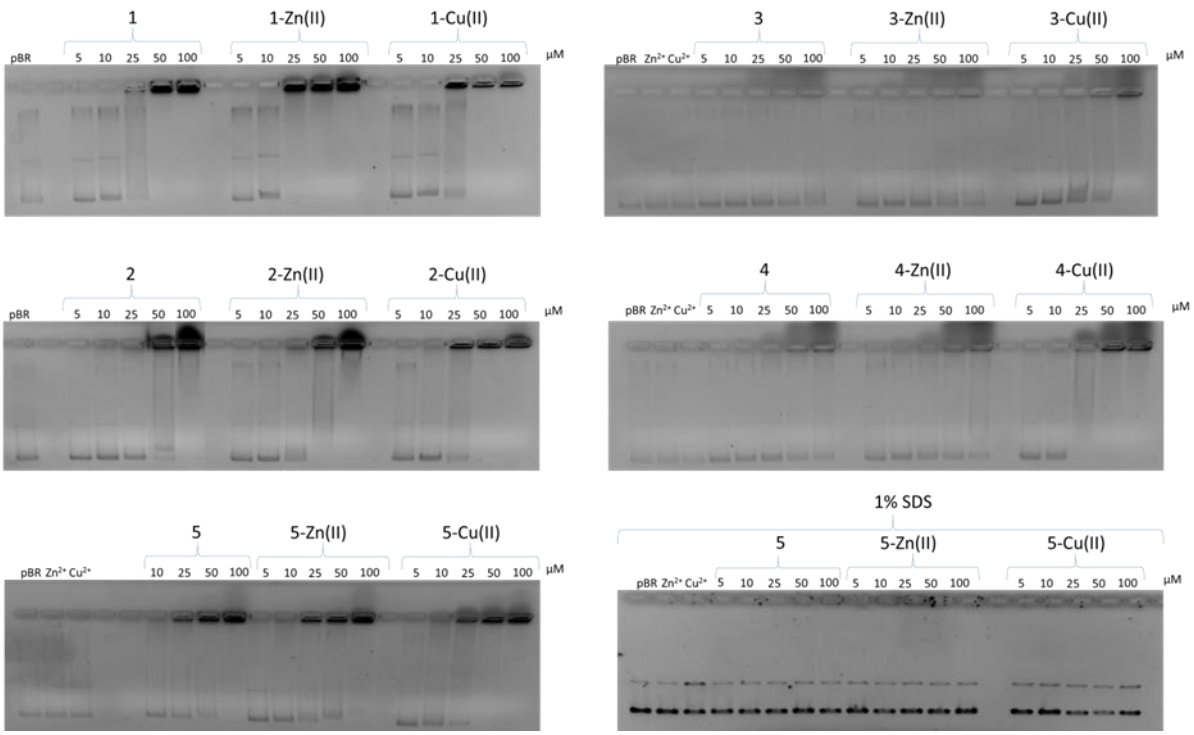

Figure 4. Agarose gel electrophoresis of pBR 322 DNA (24 μM) after 30 min incubation at 37°C with the indicated concentration of ligands **1**-**5** and the corresponding Zn(II) or Cu(II) complexes in 20 mM HEPES, pH 7.1. The panel at the bottom on the right refers to samples added of 1% SDS before loading. Zn(II) and Cu(II) lanes correspond to plasmid treated with 100 μM metal ion.

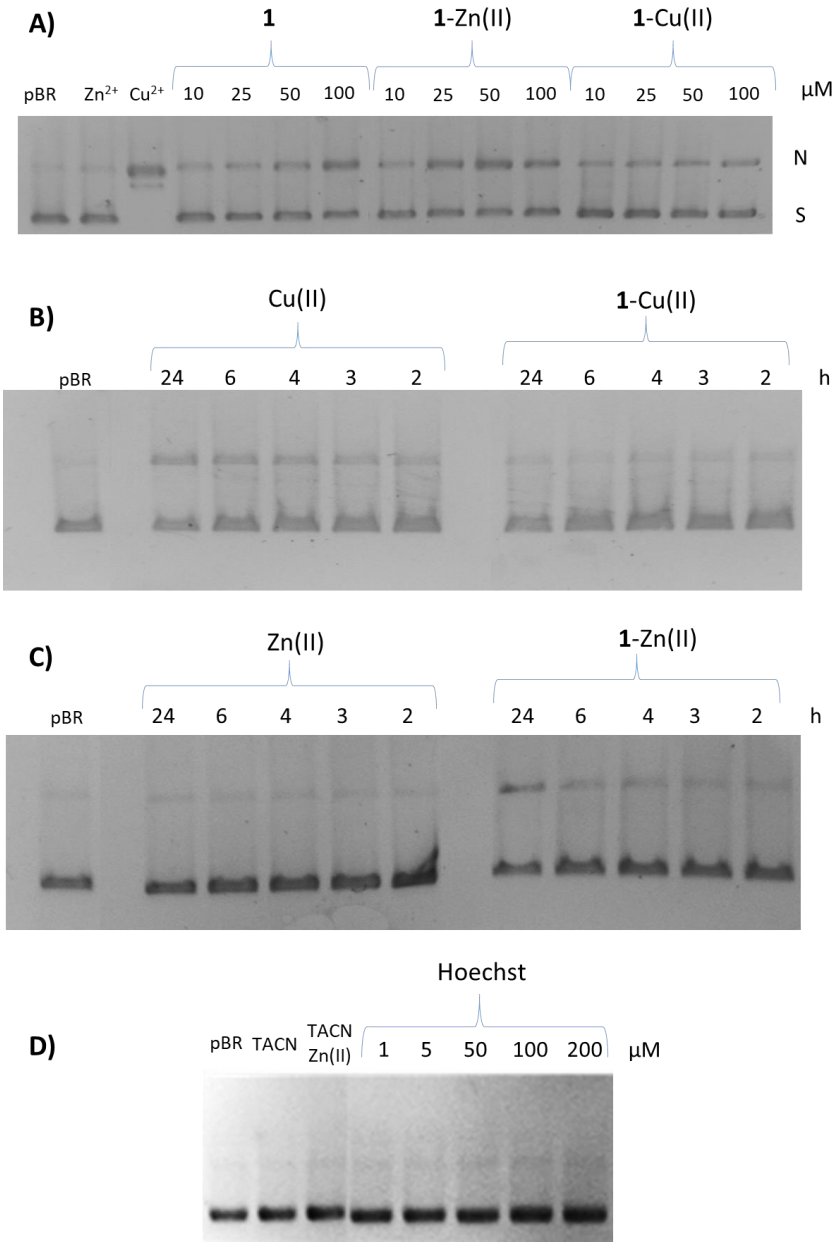

Figure 5. Panel A: Agarose gel electrophoresis of pBR 322 DNA (24 μM) after 24 h incubation at 37 °C with the increasing concentration of **1**, **1**-Zn(II) or **1**-Cu(II) in 20 mM HEPES, pH 7.0. In panels B and C, the plasmid was incubated for variable time with 15 μM metal complexes at 37 °C. In Panel D the plasmid was incubated with TACN (100 μM), TACN-Zn(II) (100 μM) and TACN-Zn(II) (100 μM) with increasing concentration of Hoechst. Before loading, all samples were added of 1% SDS. S and N refer to the supercoiled and nicked plasmid DNA, respectively. Zn(II) and Cu(II) lanes correspond to plasmid treated with 100 μM metal ion.

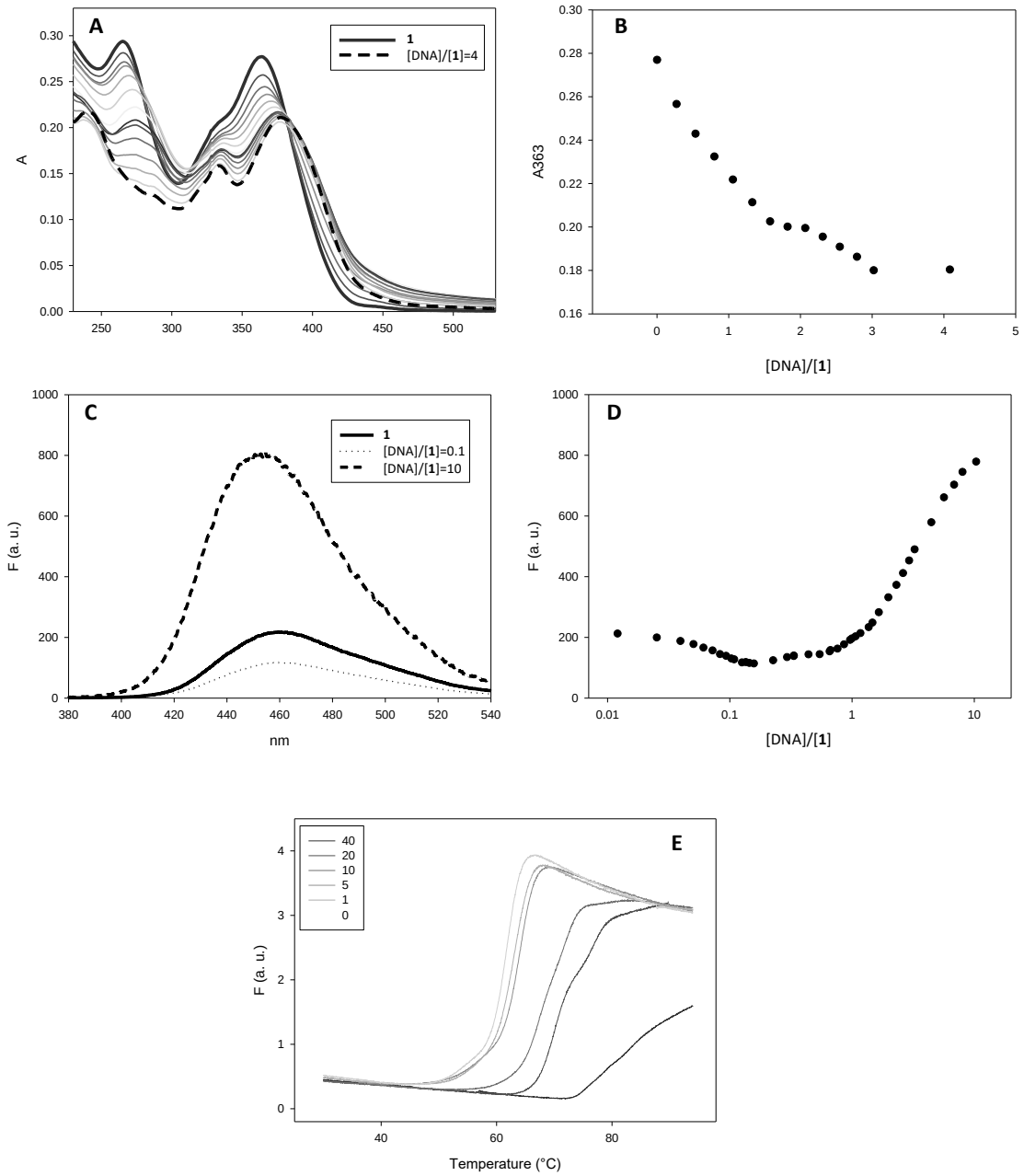

Figure 6. Variation of the absorption (Panel A) or fluorescence spectra (λ_{ecc} = 356 nm, Panel C) of **1** (15 and 2 μM, respectively) induced by the addition of ctDNA in 20 mM HEPES, 50 mM NaCl, pH 7.1. Bold solid and dashed lines correspond to the spectra of the free and fully bound **1**, respectively. In Panel B and D the relative variation of the absorbance or fluoresce recorded at 363 or 460 nm is reported as a function of the nucleic acid/ligand molar ratio. In Panel E the denaturation profiles of a FAM-labelled dsDNA fragment in the presence/absence of increasing **1** concentration (the concentration of 1 is given in the inset in micromolar units).

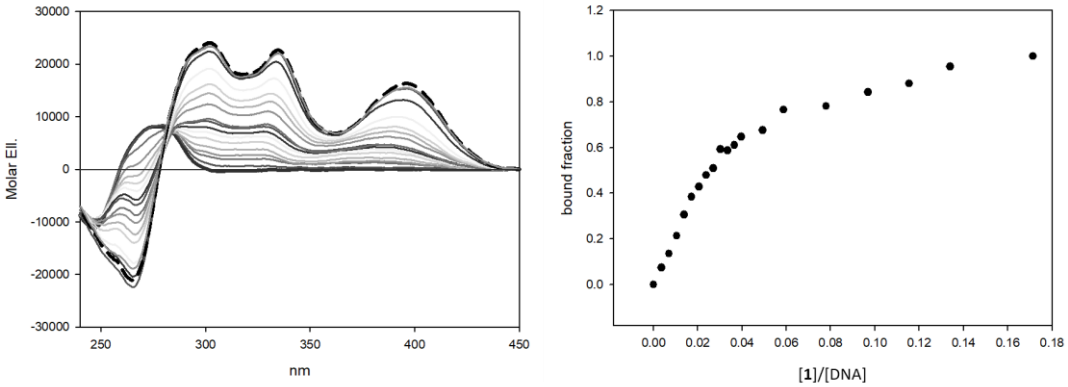

Figure 7. CD spectra of 88 μM ctDNA alone and in the presence of increasing concentrations of **1** recorded in 20 mM HEPES, pH 7.1. Bold solid and dashed lines correspond to the spectra of the free and fully bound **1**, respectively.

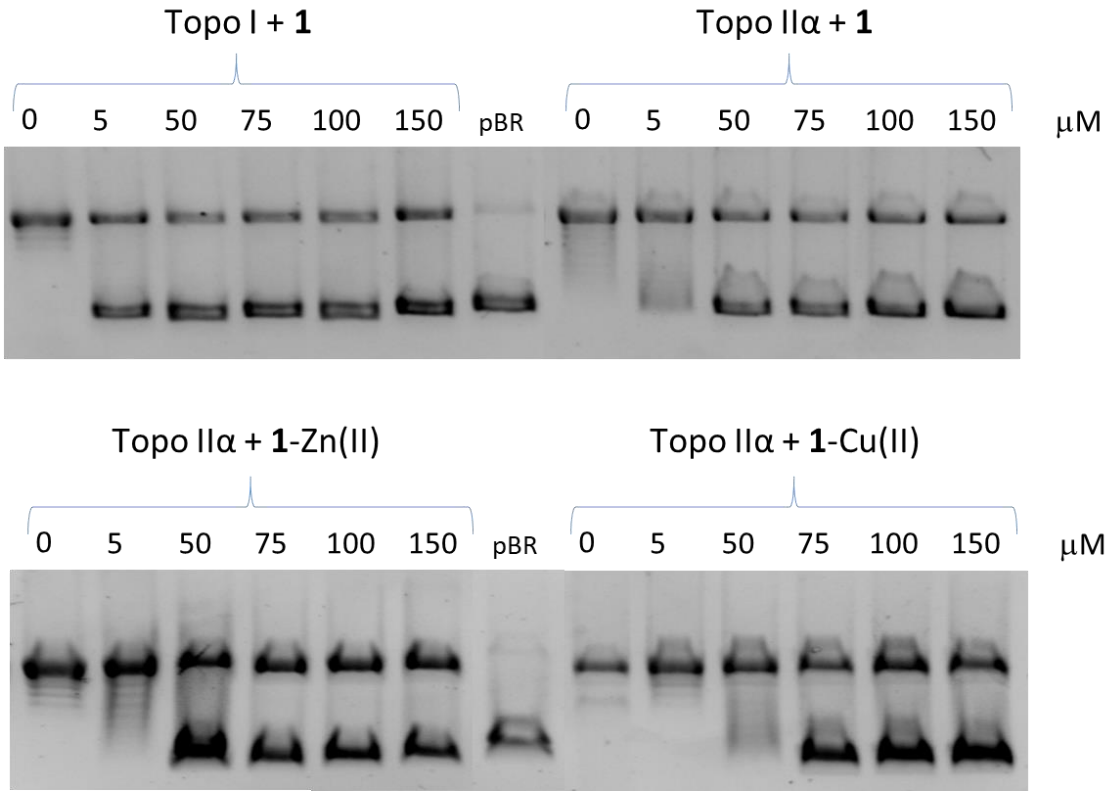

Figure 8. Agarose gel electrophoresis of pBR322 DNA (0.125 μg) in the presence/absence of 1 U of human topoisomerase I or IIα after 1 h incubation at 37 °C with increasing concentration of **1**, **1**-Zn(II) or **1**-Cu(II) in reaction buffer 1X.